

Accepted Manuscript

Synthesis, characterization, monoamine oxidase inhibition, molecular docking and dynamic simulations of novel 2,1-benzothiazine-2,2-dioxide derivatives

Shakeel Ahmad, Sumera Zaib, Saquib Jalil, Muhammad Shafiq, Matloob Ahmad, Sadia Sultan, Mazhar Iqbal, Sana Aslam, Jamshed Iqbal

PII: S0045-2068(18)30099-3
DOI: <https://doi.org/10.1016/j.bioorg.2018.04.012>
Reference: YBIOO 2335

To appear in: *Bioorganic Chemistry*

Received Date: 3 February 2018
Revised Date: 13 April 2018
Accepted Date: 17 April 2018

Please cite this article as: S. Ahmad, S. Zaib, S. Jalil, M. Shafiq, M. Ahmad, S. Sultan, M. Iqbal, S. Aslam, J. Iqbal, Synthesis, characterization, monoamine oxidase inhibition, molecular docking and dynamic simulations of novel 2,1-benzothiazine-2,2-dioxide derivatives, *Bioorganic Chemistry* (2018), doi: <https://doi.org/10.1016/j.bioorg.2018.04.012>

This is a PDF file of an unedited manuscript that has been accepted for publication. As a service to our customers we are providing this early version of the manuscript. The manuscript will undergo copyediting, typesetting, and review of the resulting proof before it is published in its final form. Please note that during the production process errors may be discovered which could affect the content, and all legal disclaimers that apply to the journal pertain.



Synthesis, characterization, monoamine oxidase inhibition, molecular docking and dynamic simulations of novel 2,1-benzothiazine-2,2-dioxide derivatives

Shakeel Ahmad^{a,‡}, Sumera Zaiib^{b,‡}, Saquib Jalil^b, Muhammad Shafiq^a, Matloob Ahmad^{a,*},
Sadia Sultan^{c,d}, Mazhar Iqbal^e, Sana Aslam^f, Jamshed Iqbal^{b,*}

^aDepartment of Chemistry, Government College University, Faisalabad-38000, Pakistan.

^bCentre for Advanced Drug Research, COMSATS Institute of Information Technology, Abbottabad-22060, Pakistan.

^cFaculty of Pharmacy, Universiti Teknologi MARA, Puncak Alam Campus, 42300 Bandar Puncak Alam, Selangor Darul Ehsan, Malaysia.

^dAtta-ur-Rahman Institute for Natural Products Discovery (AuRIns), Universiti Teknologi MARA, Puncak Alam Campus, 42300 Bandar Puncak Alam, Selangor Darul Ehsan, Malaysia.

^eDrug Discovery and Structural Biology Group, Health Biotechnology Division, National Institute for Biotechnology and Genetic Engineering, Faisalabad 38000, Pakistan.

^fDepartment of Chemistry, Government College Women University, Faisalabad-38000, Pakistan.

[‡]These authors contributed equally.

Correspondence:

Prof. Dr. Jamshed Iqbal, Centre for Advanced Drug Research, COMSATS Institute of Information Technology, Abbottabad, Postal Code-22060, Pakistan, Tel: +92-992-383591-96, Fax: +92-992-383441, E-Mail: drjamshed@ciit.net.pk / jamshediqb@googlemail.com

Dr. Matloob Ahmad, Department of Chemistry, Government College University, Faisalabad-38000, Pakistan, Email: matloob.ahmad@gcuf.edu.pk / matloob_123@yahoo.com

Abstract

In this research work, we report the synthesis and biological evaluation of two new series of 1-benzyl-4-(benzylidenehydrazono)-3,4-dihydro-1*H*-benzo[*c*][1,2]thiazine 2,2-dioxides and 1-benzyl-4-((1-phenylethylidene)hydrazono)-3,4-dihydro-1*H*-benzo[*c*][1,2]thiazine 2,2-dioxides. The synthetic plan involves the mesylation of methyl anthranilate with subsequent *N*-benzylation of the product. The methyl 2-(*N*-benzylmethylsulfonamido)benzoate was subjected to cyclization reaction in the presence of sodium hydride to obtain 1-benzyl-1*H*-benzo[*c*][1,2]thiazin-4(3*H*)-one 2,2-dioxide which was treated with hydrazine hydrate to get

corresponding hydrazone precursor. Finally, the titled compounds were obtained by reaction of hydrazone with various substituted aldehydes and ketones. The synthesized derivatives were subjected to carry out their inhibition activities against monoamine oxidases along with modelling investigations to evaluate their binding interactions and dynamic stability during the docking studies. The inhibition profile of potent compounds was found as competitive for both the isozymes. The compounds were more selective inhibitors of MAO-A as compared to MAO-B. Moreover, drug likeness profile of the derivatives was evaluated to have an additional insight into the physicochemical properties. The molecular dynamic simulations predicted the behaviour of amino acids with the active site residues.

Keywords: 2,1-Benzothiazine 2,2-dioxides, Hydrazones, monoamine oxidases, molecular dynamic simulations, docking studies

1. Introduction

Monoamine oxidase (MAO) is a FAD-dependent oxidoreductase enzyme found in the mitochondrial outer membrane of neurons, glia and other mammalian tissue cells, such as kidney, liver, glandular cells and intestinal epithelium [1,2]. Two isoenzymes of MAO have been identified and distinguished (MAO-A and MAO-B), both have ~ 70% sequence identity, having non-similar behaviour in their tissue distribution along with substrate and inhibitor specificity [3,4]. MAO-A is a ubiquitous MAO isoform, that plays an important role in the deactivation of neurotransmitter, dietary and xenobiotic amines, such as serotonin (5-HT), norepinephrine, tyramine and dopamine and its selective inhibitor is clorgyline [5,6], while, MAO-B predominantly exists in brain and helps in the metabolism of dopamine and β -phenylethylamine, an endogenous amine which promotes dopamine release by inhibiting the neuronal reuptake, and is inhibited selectively by selegiline [5,6].

Selective MAO-A inhibitors have shown to be effective against anxiety and depression [7], whereas, selective inhibitors of MAO-B are useful in the treatment of several neurodegenerative diseases, like Parkinson's disease (PD) and Alzheimer's disease (AD) [8]. The increased levels of monoamine oxidases results in elevated production of hydrogen peroxide, a by-product which is responsible for enhancing the level of reactive oxygen species (ROS) [1,4]. These ROS are mainly involved in the pathogenesis of neurodegenerative diseases. Therefore, monoamine inhibitors are feasible and potential drug target for neurodegenerative diseases as they are involved in the prevention of oxidative

damage in addition to their role as antidepressant (MAO-A) and neuroprotective (MAO-B) agents [1,4].

The level of monoamine oxidase increases in the brain of human species during aging and the oxidative stress which is a potential risk factor for neuronal damage and also causes death in aging and age related neurodegenerative disorders like AD and PD [9-11]. Selective inhibitors of monoamine oxidase are therefore considered as a significant therapeutic option for these disorders so that the level of metabolic degradation of dopamine can be reduced. Thus, selegiline (deprenyl), rasagiline (Figure 1), two irreversible MAO-B inhibitors, are commonly used for symptomatic treatment of PD [12]. Another MAOI-B, safinamide (Figure 1), was recently approved in the European Union (EU) for the treatment of PD [13]. In fact, the interest in selective inhibitors of monoamine oxidase has increased in the last several years, due to their therapeutic potential for neurodegenerative disorders and other pathologies in which enzyme is involved [14,15]. The research in the area evolved significant number of several derivatives based on variety of oxygen, sulphur and nitrogen containing compounds [16-27].

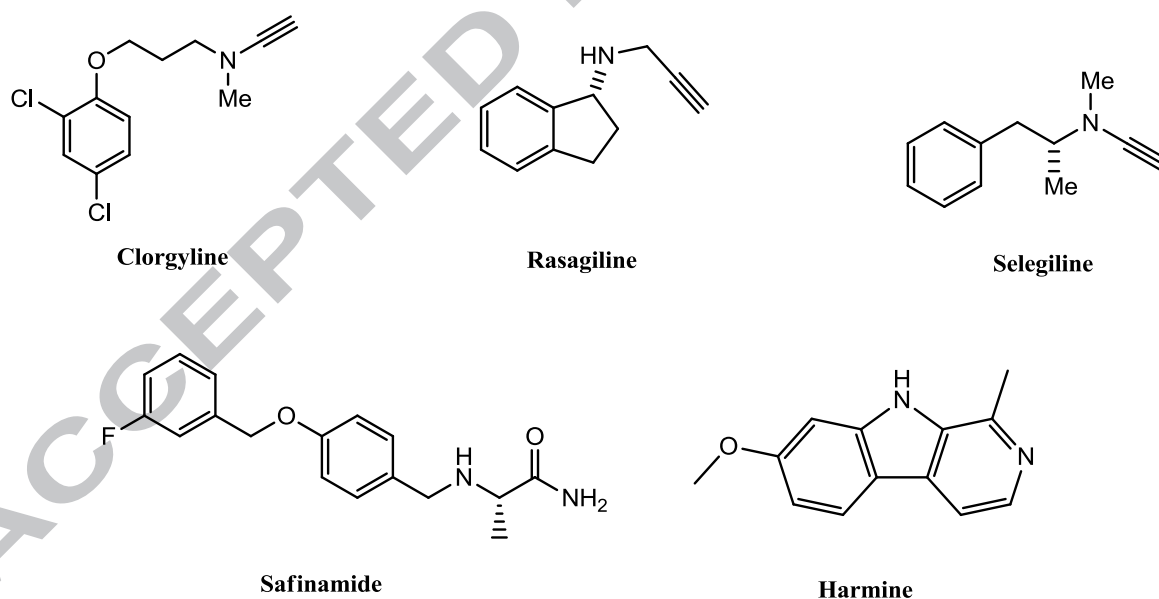


Figure 1. Structures of some clinically used MAO inhibitor drugs.

One of the main goals of synthetic organic chemistry is the discovery of novel and effective therapeutic agents. Benzothiazines constitutes a very important class of heterocyclic compounds, possessing diversified biological activities such as antiviral (reverse transcriptase

inhibitors) [28], antimalarial [29] and antibacterial activities [30]. The hydrazone derivatives, *N*-benzylidene-*N'*-(1-methyl-2,2-dioxo-2,3-dihydro-1*H*-2λ6-benzo[*c*][1,2]thiazin-4-ylidene)-hydrazines are reported as antibacterial agents [31]. The benzo[2,1]thiazine-4(3*H*)-one 2,2-dioxide core is bioisosteric to the benzo[1,2]thiazine-4(3*H*)-one which served as a precursor for oxicams *i.e.*, piroxicam, droxicam and meloxicam *etc* [32]. 2,1-Benzothiazine derivative, ethyl 2-(2-(4-hydroxy-1-methyl-2,2-dioxido-1*H*-benzo[*c*][1,2]thiazine-3-carboxamido)thiazol-4-yl)acetate (**1**) exhibited better analgesic character (Figure 2) as compared to oxicam drugs, piroxicam (**2**) and meloxicam (**3**) [33]. Various other derivatives of 2,1-benzothiazine-2,2-dioxide displayed their ability as lipoxygenase inhibition [34], treatment for a variety of heart diseases [34], chiral ligands [35], antipsychotic [36] anti-inflammatory [37] and anticonvulsant [38]. Moreover, several benzothiazine derivatives have been reported as anticancer [39], CD73 inhibitors [40], analgesic [41] and neuroprotective agents [42] and also act as modulator of pro- and anti-inflammatory cytokines in rheumatoid arthritis [43].

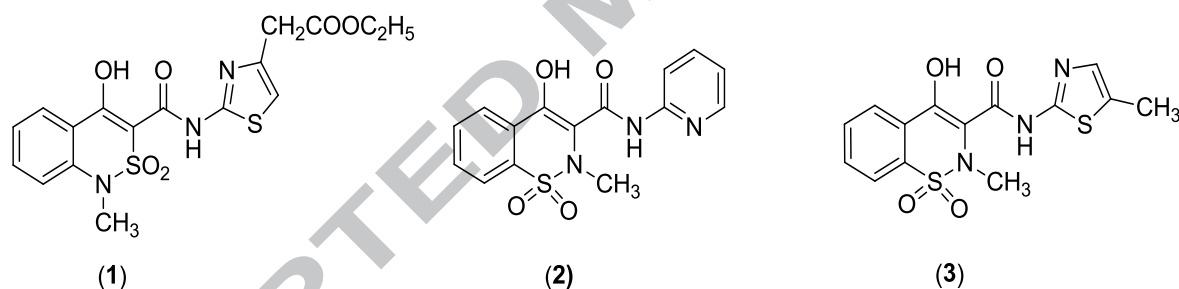


Figure 2. Structures of benzothiazine based analgesic agents

In the present study, taking into account of our previous work [22-27], three new series of novel 2,1-benzothiazine-2,2-dioxide derivatives have been designed, synthesized and evaluated as monoamine oxidase inhibitors. To investigate the abilities of the synthesized compounds to access the brain, their permeation across the blood-brain barrier has been theoretically investigated and predicted *in silico*. Moreover, the docking studies were carried out for binding interaction comparison and the dynamic simulation studies were performed to monitor the behaviour of amino acid with potent compounds inside the active site.

2. Results and Discussion

2.1. Chemistry

The synthetic route for the novel series of hydrazine derivatives of 2,1-benzothiazine-2,2-dioxide is shown in the Scheme 1. First of all mesylation of methyl anthranilate was carried out to get sulphonamide (**6**), which was further *N*-benzylated (**8**) and then cyclized to obtain 1-benzyl-1*H*-benzo[*c*][1,2]thiazin-4(3*H*)-one 2,2-dioxide (**9**). The benzothiazine precursor (**9**) was further reacted with hydrazine monohydrate to synthesize corresponding hydrazone precursor (**10**), which was then condensed with a series of aromatic aldehydes, acetophenones and heterocyclic ketones to get the target compounds. The compounds were characterized by spectroscopic techniques. The SO₂CH₂ moiety in thiazine ring was observed in the range of 5 to 5.2 (δ, ppm) for the benzylidene derivatives while for phenyl ethylidene derivatives, it appeared in the shift value of 4-5 ppm. Moreover, PhCH₂ protons were observed in the shift value of 5 to 5.3 ppm. The characteristic singlet for CH=N was observed for benzylidene derivatives in the range of 8.61 to 8.96 (δ, ppm) while C(Me)=N protons for phenyl ethylidenes were observed in the range of 2.29 to 2.48 (δ, ppm) in ¹H NMR spectra. The molecular ion peaks in the mass spectrometry experiments were in well agreement to the assigned structures. Moreover, the phenomenon of tautomerism (Figure 3) was observed in the ¹H NMR of benzylidene derivatives with the appearance of NH peaks in the range of 10.49 to 11.08 (δ, ppm) and corresponding CH peaks in the shift value of 5.19 to 5.22 (δ, ppm).

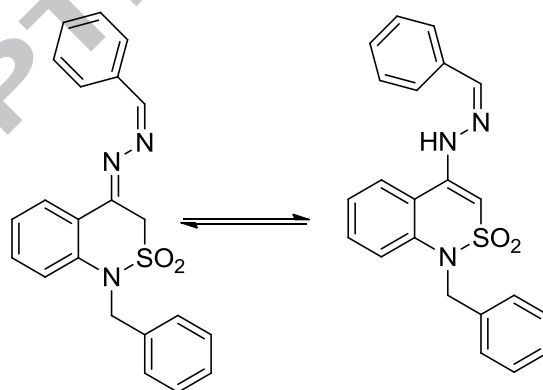
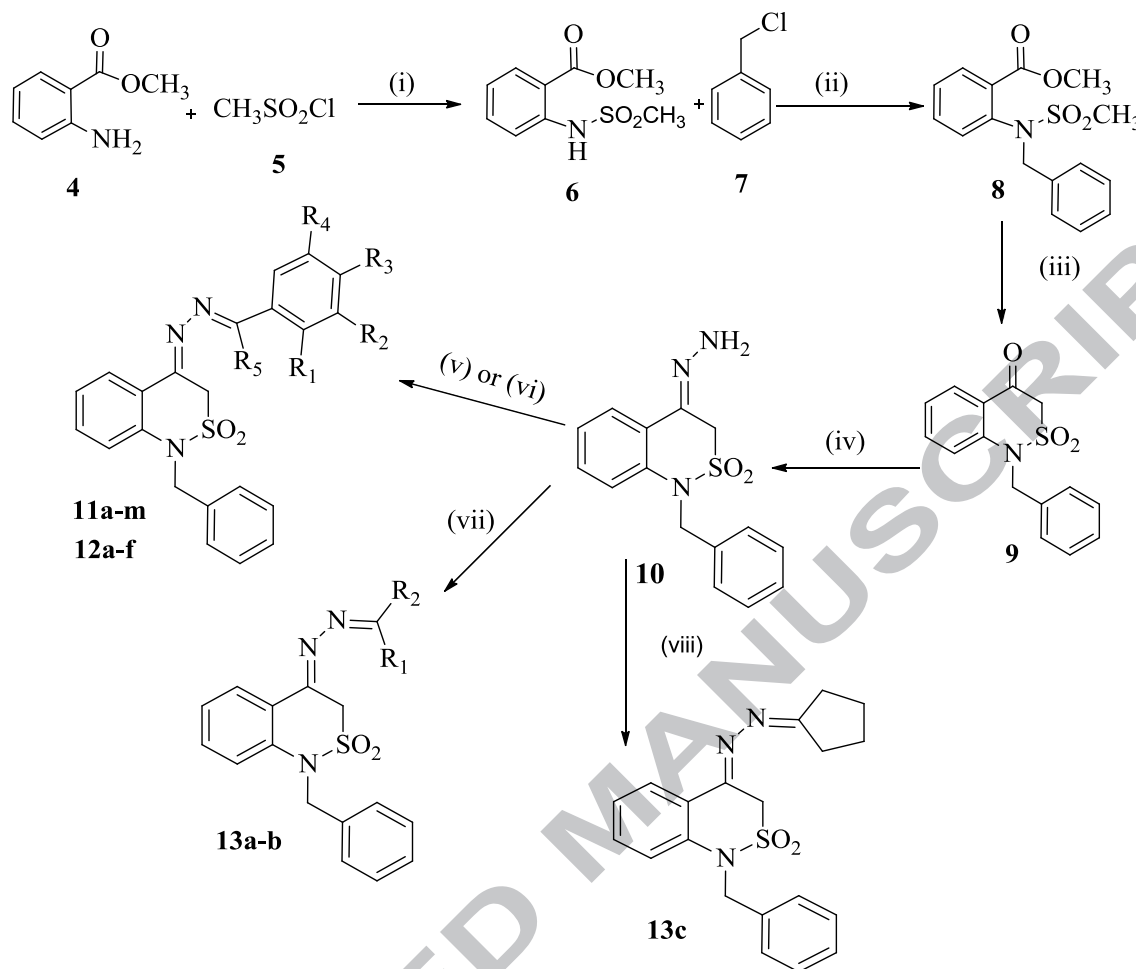


Figure 3. Tautomeric structures of benzylidene derivatives



Chemicals and Reagents: (i) DCM, TEA (ii) R-Cl, K_2CO_3 , DMF (iii) NaH, DMF (iv) $N_2H_4 \cdot H_2O$, MeOH (v) Substituted Benzaldehydes, MeOH (vi) Substituted acetophenones, MeOH (vii) 1-(pyridin-2-yl)ethanone, 1-(furan-2-yl)ethanone, MeOH (viii) Cyclopentanone, MeOH

Scheme 1. Synthetic lay out of 1-benzyl-1H-benzo[c][1,2]thiazin-4(3H)-one 2,2-dioxide and its hydrazone derivatives.

2.2. Monoamine oxidase inhibition studies

All the synthesized compounds were evaluated for their inhibitory potential against rat MAO-A and MAO-B enzymes. Clorgyline and deprenyl were used as standard inhibitors of MAO-A and MAO-B, respectively. The IC_{50} values and selectivity index (SI for IC_{50} of MAO-A over IC_{50} of MAO-B) for all the evaluated compounds and reference inhibitors were summarized in Table 1. Selectivity for MAO-A increases as the selectivity index decreases, while, selectivity towards MAO-B isoform increases as the SI increases. All compounds exhibited excellent MAO inhibition in the lower micromolar range. By investigating the

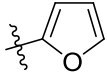
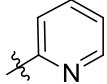
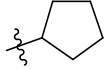
MAO-A and MAO-B inhibition potencies of the synthesized benzothiazine-2,2-dioxide derivatives, it was noticed that the unsubstituted benzothiazines (**11a**) showed significant inhibition towards MAO-A and MAO-B. Few compounds were found as dual inhibitors of MAO-A and MAO-B, and were able to inhibit both enzymes efficiently. Most of the compounds were selective toward MAO-B, while few were selective towards MAO-A.

The most potent inhibitor of monoamine oxidase A was **11i**, 1-benzyl-4-((2-bromobenzylidene)hydrazono)-3,4-dihydro-1*H*-benzo[*c*][1,2]thiazine 2,2-dioxide, having an IC_{50} value of $0.12 \pm 0.02 \mu\text{M}$, while, the potent inhibitor of monoamine oxidase B was **12d**, 4-((1-(2-aminophenyl)ethylidene)hydrazono)-1-benzyl-3,4-dihydro-1*H*-benzo[*c*][1,2]thiazine 2,2-dioxide, with an IC_{50} value of $0.13 \pm 0.08 \mu\text{M}$. However, the potent inhibitor against MAO-A, **11i** presented ~ 27 fold increased inhibition potential when compared with standard inhibitor (clorgyline, $0.0045 \pm 0.0003 \mu\text{M}$) and **12d**, MAO-B inhibitor, possess ~ 7 times less inhibitory profile than standard inhibitor deprenyl ($0.0196 \pm 0.001 \mu\text{M}$). Several other derivatives exhibited significant inhibitory activities towards monoamine oxidase A, which included **11b**, **11m**, **11g** and **13b**. However, some compounds possessed selective inhibition for monoamine oxidase B, like **11d**, **11k**, **12a** and **12b**. Some of the synthetic compounds were found dual inhibitors of both the enzymes, **11a**, **11c**, **11f**, **11h** and **11j**, and were active against monoamine oxidase A as well as monoamine oxidase B.

The K_i values for MAO-A and MAO-B were reported in nano molar concentration. The value ranges from 34.2 – 14914.2 nM for MAO-A, whereas, the value 57.5 – 33955.5 nM was found against MAO-B. However, clorgyline (standard inhibitor, MAO-A) presented K_i value of 1.28 nM, and deprenyl (standard inhibitor, MAO-B) exhibited inhibition constant of 8.711 nM. The potent inhibitor (**11i**) of MAO-A showed 34.2 nM, whereas, MAO-B selective inhibitor (**12d**) had 57.5 nM. The values were presented in Table 1.

Table 1. Structural parameters and *in-vitro* monoamine oxidase inhibition of synthesized compounds **11(a-m)**, **12(a-f)** and **13(a-c)**

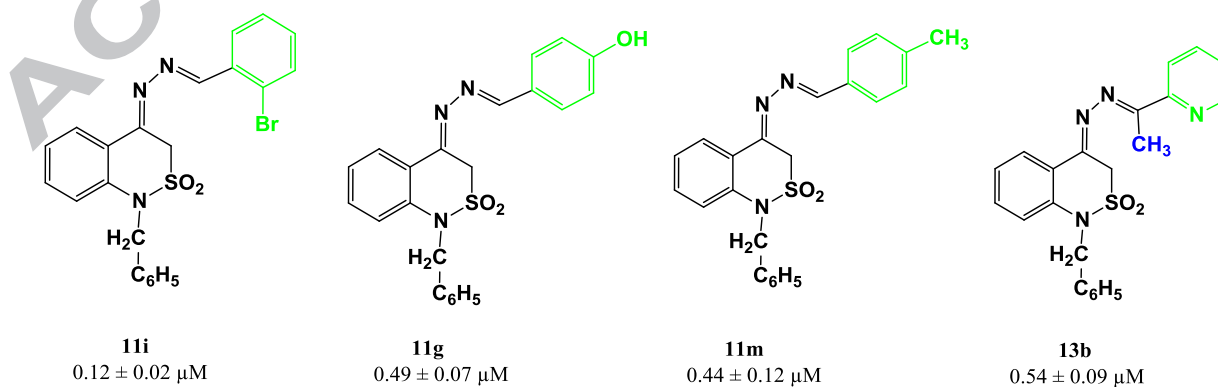
Compound codes	R ₁	R ₂	R ₃	R ₄	R ₅	MAO-A	MAO-B	K _i (nM)	
						IC ₅₀ ± SEM ^a (μM)			
11a	H	H	H	H	H	0.25 ± 0.06	0.66 ± 0.01	71.42	293.3
11b	Cl	H	H	H	H	1.87 ± 0.09	14.1 ± 0.06	534.3	6266.6
11c	H	H	Cl	H	H	0.22 ± 0.04	0.18 ± 0.03	62.85	80.0
11d	H	OCH ₃	OH	H	H	2.58 ± 0.06	0.31 ± 0.02	737.1	137.7
11e	NO ₂	H	H	H	H	20.6 ± 0.02	1.61 ± 0.09	5885.7	715.5
11f	H	OH	H	H	H	0.46 ± 0.03	0.50 ± 0.08	131.4	222.2
11g	H	H	OH	H	H	0.49 ± 0.07	2.14 ± 0.05	140.0	951.1
11h	H	H	NO ₂	H	H	1.33 ± 0.05	1.02 ± 0.06	380.0	453.3
11i	Br	H	H	H	H	0.12 ± 0.02	3.05 ± 0.01	34.28	1355.5
11j	H	H	Br	H	H	0.19 ± 0.06	0.15 ± 0.07	54.28	66.67
11k	OH	OCH ₃	H	H	H	1.26 ± 0.04	0.14 ± 0.02	360.0	62.22
11l	H	CH ₃	H	H	H	52.2 ± 0.18	68.5 ± 0.27	14914.2	30444.4
11m	H	H	CH ₃	H	H	0.44 ± 0.12	1.38 ± 0.05	125.7	613.3
12a	H	H	F	H	CH ₃	29.9 ± 0.19	0.64 ± 0.04	8542.8	284.4
12b	Cl	H	Cl	H	CH ₃	40.0 ± 0.14	0.14 ± 0.05	11428.5	62.22
12c	OH	H	H	Cl	CH ₃	44.3 ± 0.22	41.9 ± 0.09	12657.1	18622.2
12d	NH ₂	H	H	H	CH ₃	15.5 ± 0.08	0.13 ± 0.08	4428.51	57.78
12e	H	H	Cl	H	CH ₃	1.07 ± 0.02	76.4 ± 0.11	305.7	33955.5

12f	H	H	H	H	CH ₃	3.72 ± 0.03	59.9 ± 0.13	1062.8	26622.2
13a	CH ₃		-	-	-	39.9 ± 0.19	56.8 ± 0.19	11400.0	25244.4
13b	CH ₃		-	-	-	0.54 ± 0.09	49.1 ± 0.07	154.3	21822.2
13c	H		-	-	-	5.62 ± 0.01	25.3 ± 0.05	1605.7	11244.4
Clorgyline^b	-	-	-	-	-	0.0045 ± 0.0003	61.35 ± 1.13	1.28	27266.6
Deprenyl^b	-	-	-	-	-	67.25 ± 1.02	0.0196 ± 0.001	19214.2	8.711

^aAll the values are expressed as the mean ± SEM of triplicate determinations; ^bPositive control; ^cSI = [IC₅₀ MAO-A(μM)]/[IC₅₀ MAO-B (μM)].

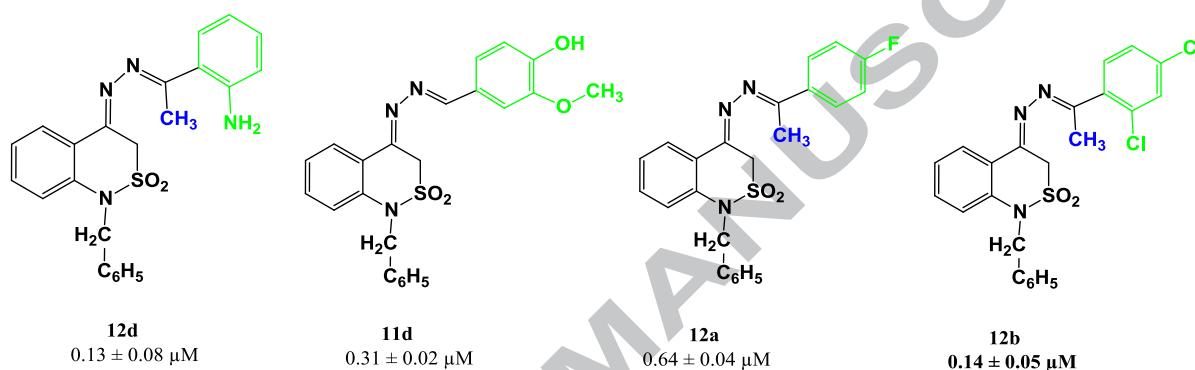
2.2.1. Structure activity relationship

The role of substitution patterns and their nature at the benzylidene ring was investigated in order to get detail information about the identification and development of selective inhibitors of monoamine oxidases. Among the three series, **11(a-m)** series derivatives showed notable contribution towards the inhibition of monoamine oxidases (A & B). When substituents were added to the basic structure, 1-benzyl-4-((*E*)-(benzylidenehydrazono)-3,4-dihydro-1*H*-benzo[*c*][1,2]thiazine 2,2-dioxide, the significant effect was noted towards monoamine oxidase A. When series having phenylethylidenehydrazono ring instead of benzylidenehydrazono ring, was taken into account, the substituent added selective inhibition profile of compounds towards monoamine oxidase B. Among the third series (**13a-c**), only potent compound was **13b**, 1-benzyl-4-((*E*)-(1-(pyridin-2-yl)ethylidene)hydrazono)-3,4-dihydro-1*H*-benzo[*c*][1,2]thiazine 2,2-dioxide, which exhibited selective inhibition for MAO-A. More specifically, when monoamine oxidase A inhibitors were examined, the structure activity relationship showed that addition of 2-bromo at benzylidene ring (**11i**) resulted in the most potent and selected inhibitor of MAO-A, presenting an IC_{50} value of $0.12 \pm 0.02 \mu\text{M}$. When inhibitory activities of other compounds were compared with the potent inhibitor, it was noted that 4-hydroxybenzylidene derivative, **11g**, showed significant inhibitory values ($0.49 \pm 0.07 \mu\text{M}$) towards MAO-A. Moreover, 4-methylbenzylidene substituted compound (**11m**) was also found as selective inhibitor of MAO-A with an inhibitory concentration of $0.44 \pm 0.12 \mu\text{M}$. The compounds **12(a-f)** did not show significant inhibitions towards monoamine oxidase A except **12e**, which showed an IC_{50} value of $1.07 \pm 0.02 \mu\text{M}$, however, among series **13(a-c)**, the compound **13b** was found as selective inhibitor of MAO-A ($0.54 \pm 0.09 \mu\text{M}$).

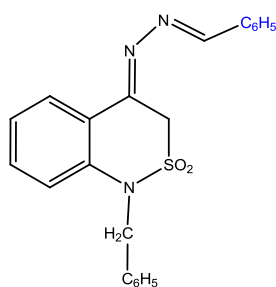


When inhibitory profile of monoamine oxidase B inhibitors was investigated, it was noticed that **12d**, 4-((1-(2-aminophenyl)ethylidene)hydrazono)-1-benzyl-3,4-dihydro-1*H*-benzo[*c*]

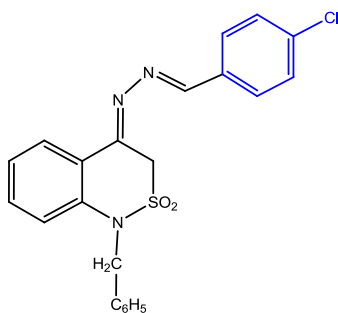
[1,2]thiazine 2,2-dioxide, was the most potent and selective inhibitor with an IC_{50} value of $0.13 \pm 0.08 \mu\text{M}$. However, other compounds of the series **12a** and **12b** were also notable and selective inhibitors of MAO-B with the inhibitory concentrations of 0.64 ± 0.04 and $0.14 \pm 0.05 \mu\text{M}$, respectively. Among series **13(a-c)**, none of the compounds exhibited notable inhibition against monoamine oxidase B. Furthermore, **11d** ($IC_{50} \pm \text{SEM} = 0.31 \pm 0.02 \mu\text{M}$), having 4-hydroxy-3-methoxybenzylidene as substituent was the active member among **11(a-m)** series. Moreover, **11k** ($IC_{50} \pm \text{SEM} = 0.14 \pm 0.02 \mu\text{M}$) was also a significant candidate when MAO-B inhibitory activity was taken into account.



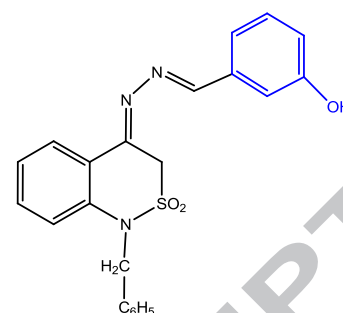
When the inhibitory activity of derivatives having dual inhibition was taken into account, few important analysis were made. The compound, **11i**, having 2-bromobenzylidene was the selective inhibitor of MAO-A, whereas, **11j**, 4-bromobenzylidene, was found as nonselective dual inhibitor for MAO-A and MAO-B. Similarly, when change in position of nitro group was noticed, the compound (**11e**) having 2-nitrobenzylidene showed less inhibition for MAO-A, and moderate inhibition for MAO-B, while 4-nitrobenzylidene (**11h**) was found as dual inhibitor. The change in position and nature of substituent had profound effect on the inhibition profile of compounds. Moreover, in case of compound **11g**, the substituent, hydroxyl group, at para-position was selective inhibitor of MAO-A with an inhibitory concentration of $0.49 \pm 0.07 \mu\text{M}$, whereas, when the same group was shifted to meta-position, **11f**, was non-selective dual inhibitor of MAO-A and MAO-B with IC_{50} values of 0.46 ± 0.03 and $0.50 \pm 0.08 \mu\text{M}$, respectively. The presence of hydroxyl group can be helpful in the formation of strong hydrogen bonding within the active site, and it can be a reason for showing dual inhibition of 11f. However, compound **12c**, having hydroxyl group at ortho-position along with chloro group as meta-substituent was weak inhibitor of MAO-A as well as MAO-B. It suggested that chloro group along with hydroxyl maybe the factor to cause decrease in inhibition. Furthermore, it was noticed that methoxy group along with hydroxyl as substituent contributed to enhance inhibitory activity towards MAO-B.



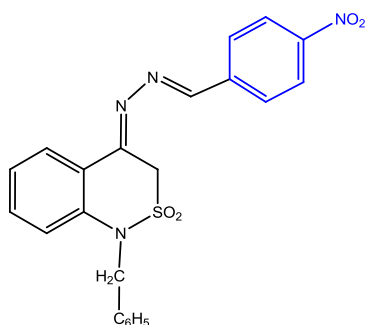
MAO-A = $0.25 \pm 0.06 \mu\text{M}$
MAO-B = $0.66 \pm 0.01 \mu\text{M}$



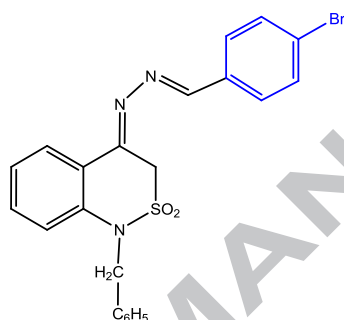
MAO-A = $0.22 \pm 0.04 \mu\text{M}$
MAO-B = $0.18 \pm 0.03 \mu\text{M}$



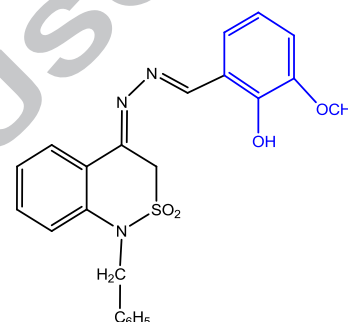
MAO-A = $0.46 \pm 0.03 \mu\text{M}$
MAO-B = $0.50 \pm 0.08 \mu\text{M}$



MAO-A = $1.33 \pm 0.05 \mu\text{M}$
MAO-B = $1.02 \pm 0.06 \mu\text{M}$



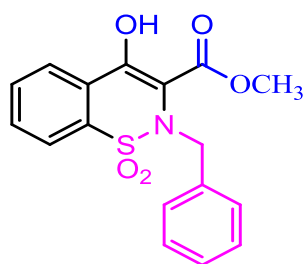
MAO-A = $0.19 \pm 0.06 \mu\text{M}$
MAO-B = $0.15 \pm 0.07 \mu\text{M}$



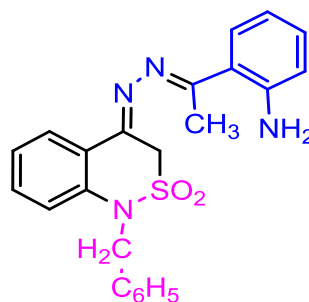
MAO-A = $1.26 \pm 0.04 \mu\text{M}$
MAO-B = $0.14 \pm 0.02 \mu\text{M}$

2.2.2. Relationship of novel compounds (benzothiazine-2,2-dioxide derivatives) with already known MAOI (benzothiazine-3-carbohydrazide 1,1-dioxides)

When relationship of the tested compound was made with already known inhibitors of monoamine oxidases, it was noted that previously reported derivatives of benzylidenethiazine-3-carbohydrazide 1,1-dioxide showed notable inhibition towards monoamine oxidases. However, recent studies were conducted to explore the inhibition effect of benzylidenethiazine 2,2-dioxide derivatives towards monoamine oxidases. The structures and their functional groups along with differences in the structures were presented below. The most interesting feature was the enhanced and selective potential of novel compounds for monoamine oxidase B. 4-((*E*)-(1-(2-aminophenyl)ethylidene)hydrazono)-1-benzyl-3,4-dihydro-1*H*-benzo[*c*][1,2]thiazine 2,2-dioxide, exhibited strong inhibition as compared to already reported inhibitor, methyl 2-benzyl-4-hydroxy-2*H*-benzo[*e*][1,2]thiazine-3-carboxylate 1,1-dioxide for MAO-B.



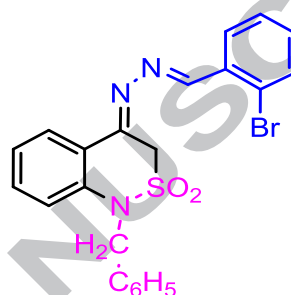
MAO-A = $0.11 \pm 0.005 \mu\text{M}$
Previous work



MAO-A = $0.12 \pm 0.02 \mu\text{M}$
This work



MAO-B = $0.21 \pm 0.01 \mu\text{M}$
Previous work



MAO-B = $0.13 \pm 0.08 \mu\text{M}$
This work

2.2.3. Kinetics Studies

In order to investigate the mode of inhibition, enzyme kinetics studies were carried out for most active inhibitors of MAO-A (**11i**) and MAO-B (**12d**). The results plotted in Figure 3 revealed that the potent compounds inhibit MAO-A and MAO-B in a competitive fashion. The Lineweaver-Burk plots of compounds **11i** and **12d** were shown in Figure 3.

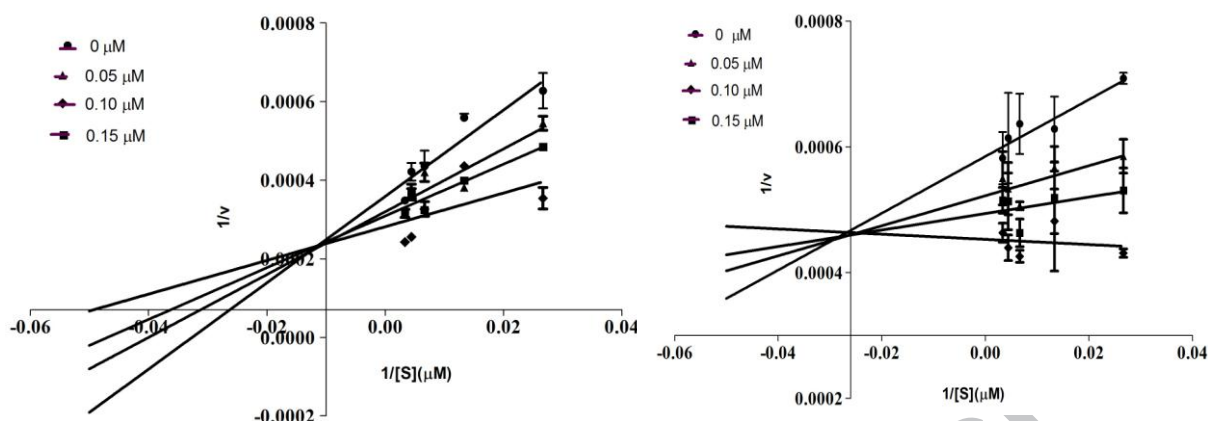


Figure 3. Lineweaver-Burk plots of MAO-A (left) and MAO-B (right) activity in the absence and presence of various concentrations of potent inhibitors, **11i** for MAO-A and **12d** for MAO-B.

2.3. Molecular docking study

2.3.1. Monoamine oxidase A

In order to justify the *in vitro* MAO inhibition results, docking study was carried out against human MAO-A (PDB ID: 2Z5Y) and MAO-B (PDB ID: 2V5Z). There were three functional domains in the active center of monoamine oxidases, the entrance cavity, the substrate cavity and the third one was aromatic cage (formed by Tyr398 and Tyr435 and FAD) [44]. For MAO-A, before docking potent compounds in the active site of the enzyme, cognate ligand harmine (7-methoxy-1-methyl-9H- β -carboline) was docked. After docking the cognate ligand successfully an RMSD value of 1.5 Å was obtained.

Amino acid residues found inside the active pocket are Tyr69, Asn181, Phe208, Val210, Gln215, Cys323, Ile325, Ile335, Leu337, Phe352, Tyr407 and Tyr444 along with cofactor flavin. For compound **11i** 1-Benzyl-4-((2-bromobenzylidene)hydrazono)-3,4-dihydro-1H-benzo[c][1,2]thiazine 2,2-dioxide, π - π interactions were observed between 3,4-dihydro-1H-benzo[c][1,2]thiazine 2,2-dioxide moiety and Tyr407 residue. The same moiety was oriented towards flavin cofactor, however, no significant interactions were observed. The 2-bromobenzylidene part was found towards amino acid residues Ile325 and Cys323. Moreover, non-covalent molecular interactions were noticed with the active site residues which are consistent to those observed previously [45]. The benzyl-4-((2-bromobenzylidene) moiety was found towards amino acid residues Ile325 and Cys323, whereas, 3,4-dihydro-1H-benzo[c][1,2]thiazine 2,2-dioxide part was deeply oriented inside the active pocket and may be the possible reason for the potential inhibition of MAO-A. The possible binding modes of

compound **11i** and the crystallographic inhibitor harmine were selected after Hyde assessment and visualization and shown in Figure 4.

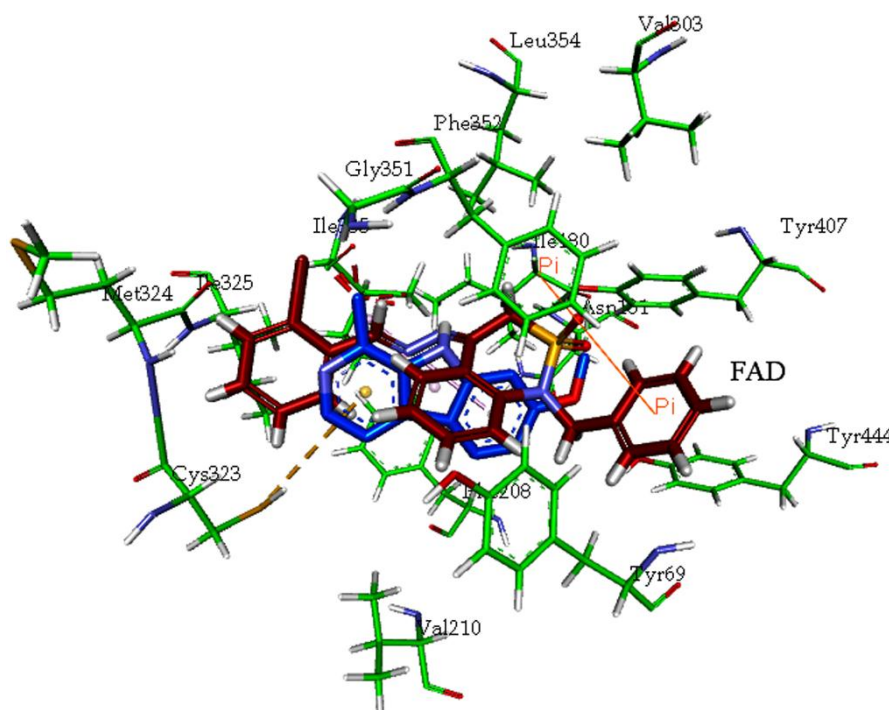


Figure 4. Possible binding mode of **11i** (brown color) and the crystallographic inhibitor harmine (blue color) bound to the active site of MAO-A

2.3.2. Monoamine oxidase B

For MAO-B, before docking the potent compounds within the active pocket of the enzyme, cognate ligand safinamide (*S*)-(+)-2-[4-(fluorobenzyloxy-benzylamino)propionamide] (SAG) was docked. After docking the cognate ligand successfully an RMSD value of 2.0 Å was obtained. MAO-B was a dimer, having globular domain monomers, which were anchored within the membrane by a C-terminal helix. In the active site of MAO-B, the substrate cavity was present towards flavin adenine dinucleotide and the entrance cavity located beneath the protein and the loop having residues 99-112 and aromatic cage were present at the end of entrance cavity [44,46]. Active site residues included Gln206, Phe103, Trp119, Ile198, Leu164, Leu167, Tyr188, Phe168, Leu171, Tyr326, Cys172, Ile199, Ile316, Tyr435, Phe343 and Tyr398 and cofactor flavin adenine dinucleotide.

The aminophenyl ethylidene ring was oriented towards flavin cofactor in the substrate cavity, while benzyl-3,4-dihydro-1*H*-benzo[*c*][1,2]thiazine 2,2-dioxide moiety was located in the entrance cavity space. Amino acid residues involved in electrostatic interactions were Phe103, Phe168, Ile198, Gln206, Tyr435, Cys172, Ile199, Tyr326 and Tyr435. Additionally, π - π interactions were observed between aminophenyl ethylidene ring and residue Tyr398 located in hydrophilic region, as hydrophilic region lies between Tyr398 and Tyr435 [47]. Figure 5 reported possible binding poses of **12d** and crystallographic inhibitor safinamide which were selected after visualization and having lowest binding energies. It was represented in the Figure 5 that 1-benzyl-3,4-dihydro-1*H*-benzo[*c*][1,2]thiazine part of compound well-occupied the entrance cavity in the same way co-crystallized ligand, safinamide had. Similarly, benzyl piperazine moiety in the substrate cavity was fitted in the same orientation as the adenine of cofactor flavin adenine dinucleotide.

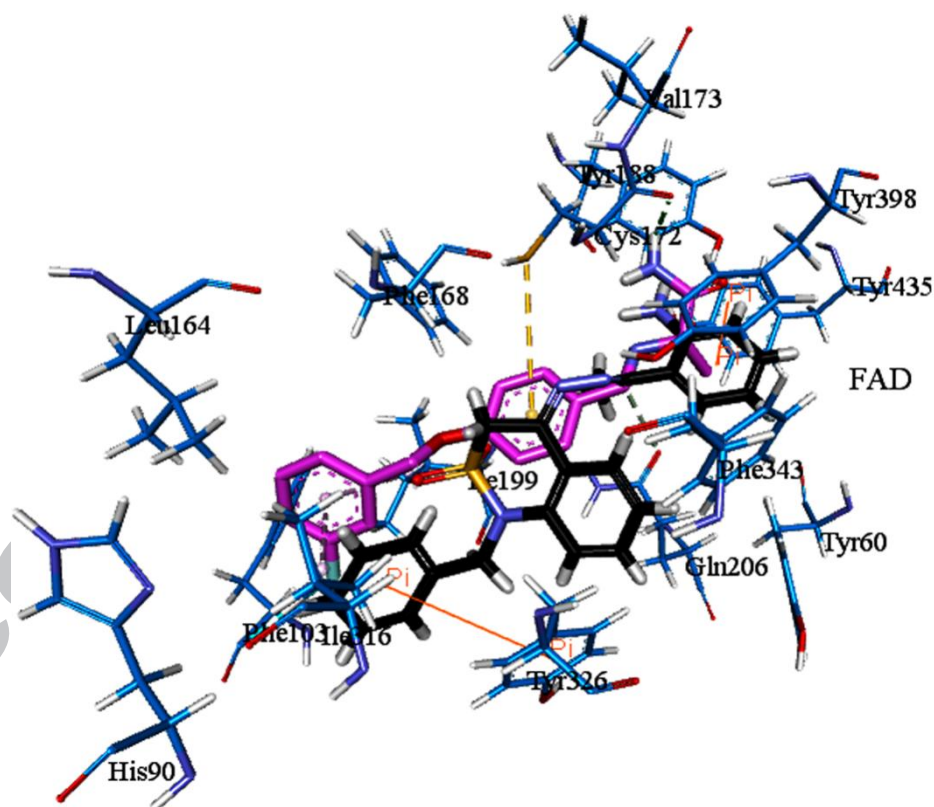


Figure 5. Possible binding mode of **12d** (black color) and the crystallographic inhibitor SAG (pink color) within the binding site of MAO-B

Moreover, the dual inhibitors, **11c** (1-benzyl-4-((4-chlorobenzylidene)hydrazono)-3,4-dihydro-1*H*-benzo[*c*][1,2]thiazine 2,2-dioxide) and **11j** (1-benzyl-4-((4-

bromobenzylidene)hydrazono)-3,4-dihydro-1*H*-benzo[*c*][1,2]thiazine 2,2-dioxide) were docked inside both the enzymes and their binding modes and interactions with the amino acids of active site were presented in Figure 6 and 7. Compound **11c** contain 4-chloro at benzylidene)hydrazono ring, whereas, 4-bromo was found at benzylidene)hydrazono in case of **11j**.

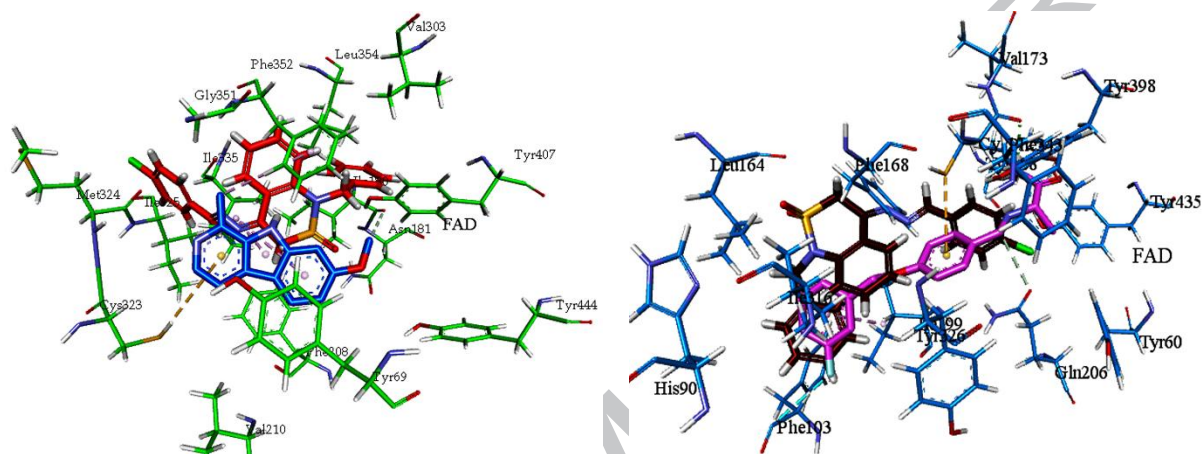


Figure 6. Possible binding mode of dual inhibitor **11c** in binding site of MAO-A (left) and in binding site of MAO-B (right) along with the respective crystallographic inhibitors

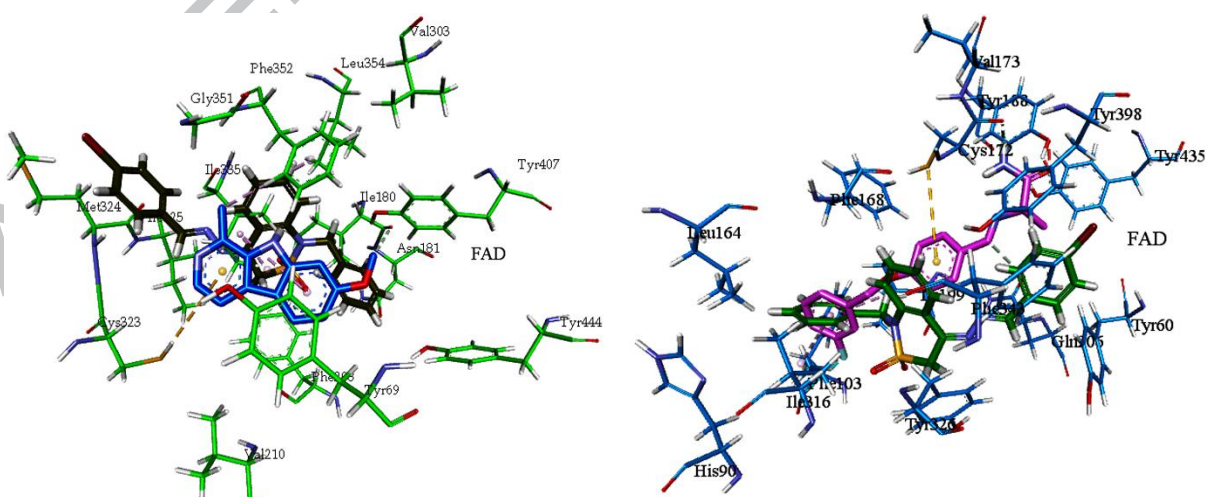


Figure 7. Possible binding mode of dual inhibitor **11j** in binding site of MAO-A (left) and in binding site of MAO-B (right) along with the respective crystallographic inhibitors

2.4. Dynamic simulation studies

Molecular dynamic simulation method was utilized to find out the transitions and conformational stability of ligand and protein. Similarly, making and breaking of different interactions between ligand and the most important amino acids within the active site were monitored during specific time frame. Dynamic simulation represented the real image of binding mode of interactions between ligand and protein. The root mean square derivation (RMSD) of the protein backbone was calculated and data was plotted against time during the molecular simulations of 5 ns for MAO-A and MAO-B were shown in Figure 8 and 9, respectively.

2.4.1. Structural stability analysis using Root Mean Square Deviation (RMSD)

In order to understand the structural and dynamic behaviour of best docked pose of the potent inhibitors and cognate ligands within the active pocket of receptors, MD simulations were done at 5 ns. In order to distinguish the effect of inhibitor on specific protein, control system was formed (free of ligand, apo) and simulated by same protocol as for ligand-protein complex (holo). Stability of the system was achieved for both the receptors and it was shown in Figure 8 and 9.

2.4.1.1. Monoamine oxidase A

During the course of evaluation, RMSD plot of MAO-A showed that in the start the system was less stable, but with the passage of time the protein and ligand start stabilizing. It was also examined that almost no change in the stability of protein-**11i** complex was found after 0.6 ns till the end of simulation *i-e.*, 5 ns. While the rest of trajectories showed little drift during the simulation time and can be noted in Figure 8. Conformational changes were observed throughout the simulation process and flexibilities were noticed in apo and holo structures. Holo structure of protein complexed with HRM and protein-**11i** were monitored. A slight jumps were observed at 2.8 ns and 4.1 ns in the trajectory of protein + **11i**, which may be due to the rotatable bonds in compound **11i**. Moreover, system was found stable when protein-HRM complex was noticed, this decrease in mobility may be due to tight binding of HRM and protein within the entrance cavity of the active site of protein.

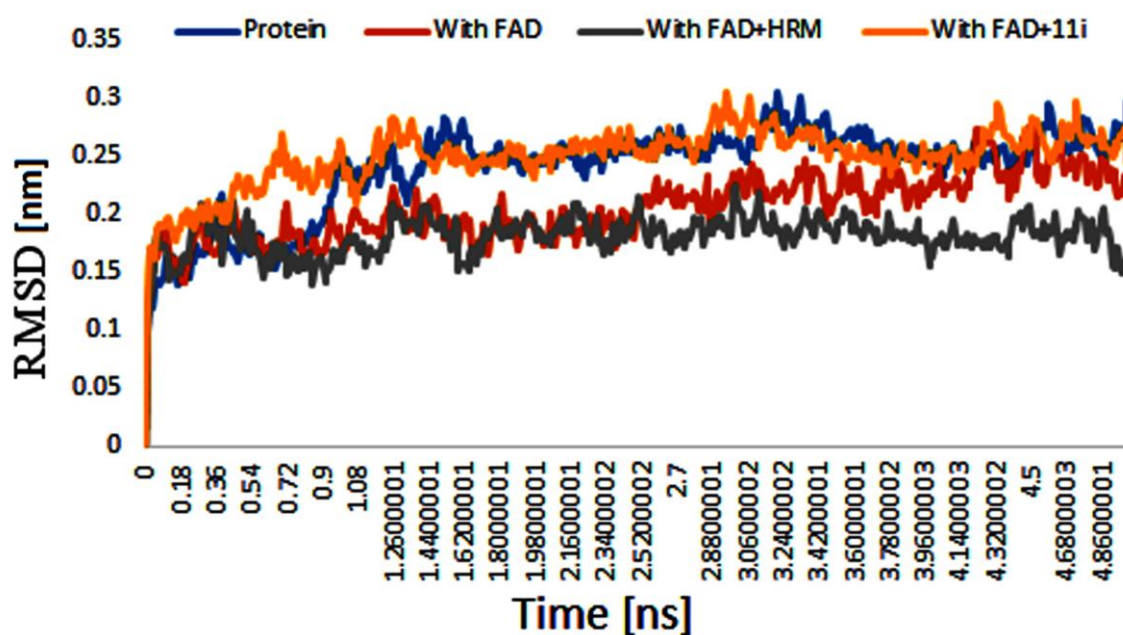


Figure 8. Evaluation of RMSD (root-mean-squared-deviation) for protein (MAO-A) backbone during the production stages of the MD simulation

2.4.1.2. Monoamine oxidase B

When RMSD plot of MAO-B was examined, the system was found in metastable state after the time frame of 900 ps. This stability started from 0.2 nm and trajectories of whole simulations, either apo (with protein only) or holo (having FAD, SAG or **12d**, the docked pose of potent inhibitor) were found to converge reasonably between 0.2-0.25 nm. No sudden jumps in trajectory of protein, protein + SAG and protein + **12d** were noticed, but due to the rotation of FAD, conformational changes were found at 1.1 and 1.6 ns. The trajectories of protein + SAG and protein + **12d** were stable at 0.2 nm throughout the simulation time, whereas, for protein + FAD, the shift was noticed between 0.25-0.30 nm, as shown in Figure 9. Protein-SAG and protein-**12d** complex are more stable as compared to protein alone, which was found to be flexible.

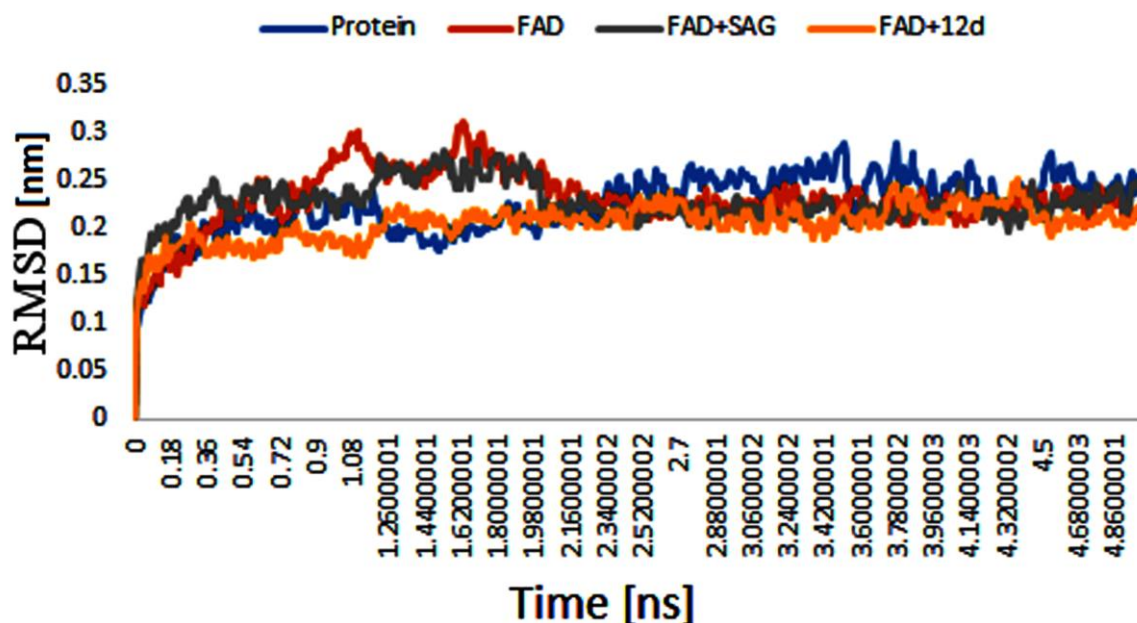


Figure 9. Evaluation of RMSD (root-mean-squared-deviation) for protein (MAO-B) backbone during the production stages of the MD simulation

2.4.2. Residue flexibility analysis using Root Mean Square Fluctuation (RMSF)

2.4.2.1. Monoamine oxidase A

Residues of both the receptors, MAO-A (PDB ID: 2Z5Y) [46] and MAO-B (PDB ID: 2V5Z) [45] were analyzed in apo state of protein and holo form, *i-e.*, in complex with FAD, cognate ligand (HRM) and the most potent compounds. The plots are represented in Figures 10 and 11 for MAO-A and MAO-B, respectively. It was illustrated from the RMSF plot of MAO-A, that residues were found stable for protein, protein with FAD alone and protein with HRM along with FAD. Whereas, when residues of **protein-11i** complex were analyzed, fluctuations at various residues were noticed. The most notable among them were with residues Ala348, Ile349, Met4350, Gly351 and at second position with residues Tyr491, Glu492, Arg493, Asn494 and Leu495. Similarly, residues Leu97, Val98, Gln99 and Tyr100 exhibited less flexibility.

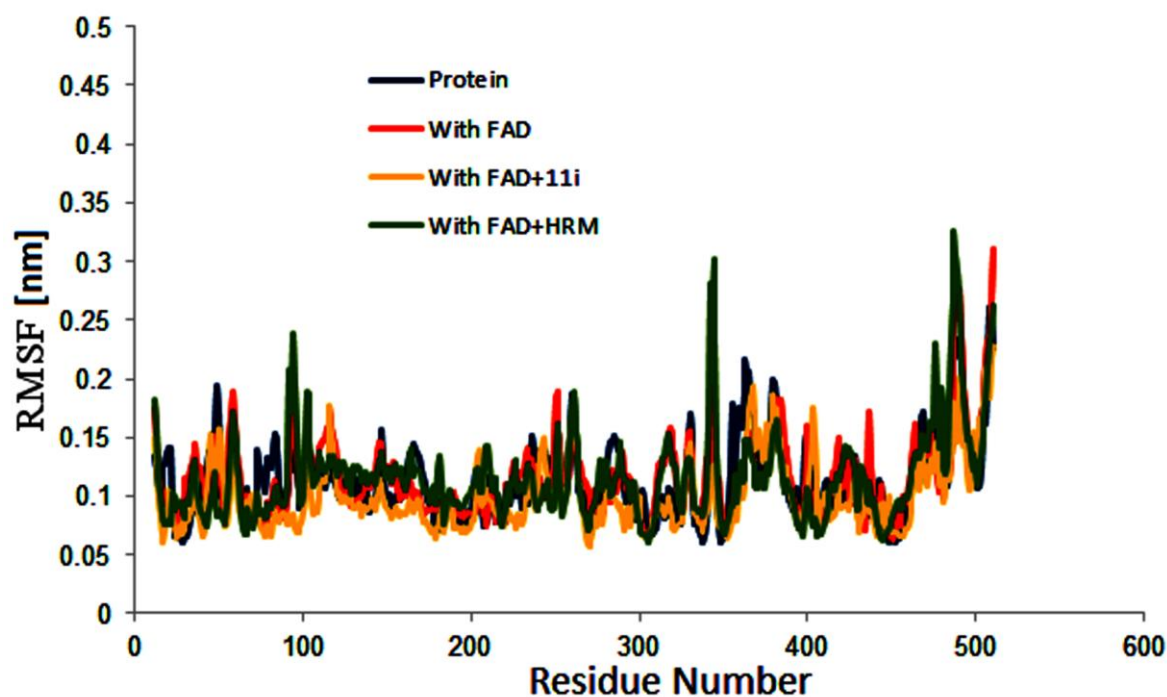


Figure 10. Root-mean-square fluctuation (RMSF) of values per residue of MAO-A during the MD simulations

2.4.2.2. Monoamine oxidase B

When root-mean-square fluctuation (RMSF) of MAO-B were examined, it was observed that residues were found stable in all the 4 simulations, *i.e.*, with protein only, protein with FAD alone, protein with **SAG** and protein with **12d** in addition to FAD. It was analysed that almost no noticeable fluctuation was seen except with terminal residues Gly497, Leu498, Thr499, Thr500 and Ile501 as shown in Figure 11.

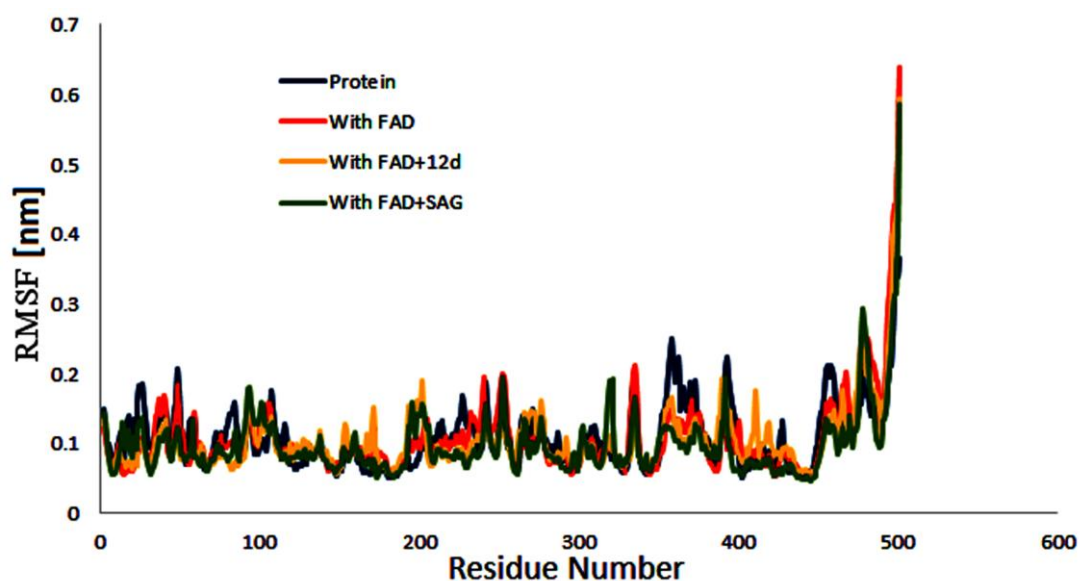


Figure 11. Root-mean-square fluctuation (RMSF) values per residue of MAO-B during the MD simulations

2.5. HYDE assessment of novel 2,1-benzothiazine-2,2-dioxide derivatives

The HYDE affinity assessment was done for the first 30 top ranking docked conformations within the active sites of monoamine oxidase A and monoamine oxidase B and it helped in the selection of correct binding mode. The binding free energy ΔG , FlexX docking score and the most favourable poses for all the synthetic derivatives **11 (a-m)**, **12 (a-f)** and **13(a-c)** were given in Table 2 (for MAO-A) & 3 (for MAO-B). Most of the compounds bind to the receptor with a very high binding affinity and give favourable contributions. Safinamide (SAG) is the co-crystallized ligand for MAO-B and by Hyde scoring showed binding free energy of -26 kJ mol^{-1} , whereas all the derivatives showed more than the binding affinity of reference ligand. Similarly, in case of MAO-A, most of the compounds bind to the receptor with a very high binding affinity as compared to the reference ligand harmine (HRM). The potent and selective inhibitors (**11i** and **12d**) presented the lowest energy scores and the binding free energies ΔG also predicted their high binding affinity inside the active pocket of respective receptors.

Table 2. Docking and Hyde scores and their corresponding ranks by Hyde affinity assessment (MAO-A)

Codes	FlexX score of the top ranking pose	Poser rank	Binding free energy ΔG (kJ mol^{-1})
-------	-------------------------------------	------------	---

11a	-12.66	1	-21
11b	-11.98	3	-18
11c	-14.92	5	-29
11d	-15.95	6	-18
11e	-16.06	27	-22
11f	-11.52	2	-25
11g	-17.39	1	-26
11h	-13.23	3	-23
11i	-19.88	4	-37
11j	-18.58	1	-20
11k	-10.81	2	-17
11l	-12.14	7	-11
11m	-11.93	6	-34
12a	-16.43	3	-26
12b	-10.16	12	-23
12c	-13.90	7	-21
12d	-18.10	8	-18
12e	-18.51	5	-16
12f	-14.38	9	-15
13a	-10.64	10	-24
13b	-16.10	4	-21
13c	-10.07	1	-19
HRM	-16.29	3	-25

Table 3. Docking and Hyde scores and their corresponding ranks by Hyde affinity assessment (MAO-B)

Codes	FlexX score of the top ranking	Poser rank	Binding free energy
	pose		ΔG (kJ mol ⁻¹)
11a	-14.95	5	-21
11b	-11.05	4	-19
11c	-15.14	1	-18
11d	-16.82	3	-26
11e	-17.93	6	-19
11f	-18.45	1	-23
11g	-14.56	2	-20
11h	-19.01	9	-28
11i	-10.19	3	-17
11j	-18.57	2	-26
11k	-19.63	4	-20
11l	-16.41	8	-14
11m	-15.32	1	-21
12a	-23.85	7	-25
12b	-21.98	5	-29
12c	-19.76	3	-22

12d	-25.92	4	-32
12e	-16.-3	6	-28
12f	-15.63	23	-19
13a	-17.43	11	-14
13b	-18.19	17	-17
13c	-15.33	3	-15
SAG	-26.13	2	-36

2.6. *In silico* physicochemical properties

Drug-likeness and *in silico* physicochemical properties for all the tested compounds were predicted using MedChem Designer3.0 [48]. Compounds having properties by which they distinguish from chemicals are identified as critical properties. These parameters work out to Lipinski's rule of five, following which, molecular weight should be less than 500 Da, calculated octanol/water partition coefficient less than five (lipophilicity), number of H-bond donors less than five and number of H-bond acceptors less than 10 [49]. Studies showed that CNS drugs possess low level of lipophilicities and less molecular weight. In addition, drugs are also characterized by low H-bond capacity and less number of rotatable bonds [50]. Herein, we determined the octanol-water distribution and partition coefficients ($S + \log D$), octanol-water partition coefficient ($S + \log P$), no. of H-bond donors (HBD), H-bond acceptor (MNO) and topological polar surface area (TPSA), an important descriptor in drug absorption. A drug having less than 60-140 Å² polar surface area, is expected to be sufficiently bio-available [51]. The partition coefficient is generally representative of distribution of drug in the body. Octanol-water partition is helpful in the estimation of hydrophobicity and hydrophilicity of any drug. Most of the synthesized compounds exhibited a narrow range of lipophilicity with some deviations. Majority of the compounds showed less than 100 Å², while only few have values within the range of 100-130 Å². Therefore, in the form of drugs, all the derivatives can easily be penetrated. Typically, compounds having molecular weight < 500, $M \log P$ value < 5 are thought to be orally bioavailable with favorable ADME profile [52-53]. All the compounds possessed molecular weight less than 500. All the compounds have equal to or less than 10 rotatable bonds. The calculated ADME properties of **11(a-m)**, **12(a-f)** and **13(a-c)** derivatives are given in Table 4.

Table 4. Calculated ADME properties of **11(a-m)**, **12(a-f)** and **13(a-c)** derivatives.

Codes	<i>M log P</i>	<i>S + log P</i>	<i>S + log D</i>	Mol. Wt.	MNO	TPSA	HBDH
11a	3.486	3.829	3.829	389.47	5	62.10	0
11b	3.969	4.338	4.338	423.924	5	62.10	0
11c	3.969	4.398	4.398	423.924	5	62.10	0
11d	2.948	3.569	3.554	435.504	7	91.56	1
11e	3.572	3.836	3.836	434.476	8	107.92	0
11f	2.982	3.647	3.642	405.478	6	82.33	1
11g	2.982	3.517	3.507	405.478	6	82.33	1
11h	3.572	4.006	4.006	434.476	8	107.92	0
11i	4.075	4.422	4.422	468.38	5	62.10	0
11j	4.075	4.445	4.445	468.38	5	62.10	0
11k	2.948	3.777	3.716	435.504	7	91.56	1
11l	3.701	4.179	4.179	403.506	5	62.10	0
11m	3.701	4.317	4.317	403.506	5	62.10	0
12a	4.075	4.371	4.371	421.496	5	62.10	0
12b	4.387	5.131	5.131	472.396	5	62.10	0
12c	3.919	4.669	4.669	453.95	6	82.33	1
12d	3.708	3.575	3.575	418.52	6	88.12	2
12e	4.180	4.603	4.603	437.95	5	62.10	0
12f	3.701	4.046	4.046	403.506	5	62.10	0
13a	2.565	3.122	3.122	393.467	6	75.24	0
13b	2.714	3.067	3.067	404.493	6	74.99	0
13c	2.99	3.137	3.137	367.472	5	62.10	0

2.7. Cytotoxic Potential by MTT Assay

In vitro evaluation of anticancer activity of all the compounds **11(a-m)**, **12(a-f)** and **13(a-c)** was carried out using the 3-(4,5-dimethylthiazol-2-yl)-2,5-diphenyltetrazolium bromide (MTT) assay. The cell viability was determined by measurement of purple formazan that was formed after metabolization of yellow colored tetrazolium bromide (MTT). This conversion of yellow tetrazolium bromide to purple formazan is brought about by oxidoreductase enzymes that are typically present in the cytosol of living cells, thereby providing an estimate of number of viable (healthy (control) and cancerous) cells present after treatment with test compounds. The screening of all the derivatives was carried out using cervical cancer cells (HeLa). The viability of cells was carried out after 24 h treatment with 100 μ M concentration of the synthetic derivatives. The cytotoxic potential was measured at the final concentration of 100 μ M of tested compounds. The obtained results are expressed as percentage of viability stated in untreated cells and are presented in Table 5. Carboplatin was used as a standard drug.

The most potent inhibitor was **11l**, with an inhibition potential of 83.8% inhibition against cervical cancer cell lines, which was followed by **13b** having 83.2%. All the synthetic derivatives presented more than 50% inhibition against cervical cancer (HeLa) which indicated that the compounds had significant inhibitory effects against cancer cell lines. Moreover, it was worth noting that all the derivatives exhibited maximum inhibition towards HeLa cells with the percentage inhibition of 60-85%.

Table 5. Cytotoxic potential of synthetic derivatives **11(a-m)**, **12(a-f)** and **13(a-c)** and standard carboplatin against cervical cancer cells (HeLa)

Compound codes	HeLa %age inhibition \pm SEM
11a	72.1 \pm 1.99
11b	76.3 \pm 1.34
11c	65.2 \pm 3.05
11d	69.7 \pm 2.49
11e	75.4 \pm 1.44
11f	82.6 \pm 2.28
11g	79.5 \pm 1.73
11h	64.8 \pm 2.12
11i	82.6 \pm 3.18
11j	71.1 \pm 2.25
11k	69.7 \pm 3.17
11l	83.8 \pm 4.36
11m	70.9 \pm 2.02
12a	78.5 \pm 1.74
12b	69.4 \pm 1.92
12c	82.2 \pm 2.34
12d	76.4 \pm 2.18
12e	69.9 \pm 3.01
12f	75.8 \pm 1.88

13a	70.1 ± 2.05
13b	83.2 ± 2.57
13c	79.3 ± 1.12
Carboplatin	84.9 ± 1.97

3. Conclusion

In summary, the present study reported an efficient synthetic plan that involved the mesylation of methyl anthranilate with subsequent *N*-benzylation of the product. The structural diversity of the synthesized derivatives was ensured by the addition of a diverse range of substituents including electron-donating and electron-withdrawing groups on the aromatic ring. The synthesized conjugates **11 (a-m)**, **12 (a-f)** and **13 (a-c)** were assayed for their monoamine oxidase inhibition potential, resulting in some highly active and selective inhibitors towards monoamine oxidase A. However, few compounds were found potent inhibitors of monoamine oxidase B. The detailed binding mode analysis with docking simulation at molecular level provided an insight into the biological properties of the analyzed compounds. Both kinetic analysis of MAO inhibition and molecular modelling study suggested that potent compound bound simultaneously to the catalytic active site of MAO-A and MOA-B. Observation of the docked poses revealed many interactions with already reported residues that effect the inhibition of MAO enzymes. These interactions were further investigated and validated through molecular simulation studies of most potent compounds. These results suggested that the inhibitors could be stabilized in the active site through the formation of multiple interactions with catalytic residues and the establishment of hydrophobic interactions in an interactive fashion. Finally, based on the activity findings and docking analysis, these compounds could potentially be developed as a novel family of structurally diverse, potent, and highly selective monoamine oxidase inhibitors. The studies revealed an interesting multi-targeted active molecules, which offer an attractive starting point for further lead optimization in the drug-discovery process against Parkinson's disease.

4. Material and methods

Please see supporting information file for material and method section.

Acknowledgements

The author, Matloob Ahmad acknowledges the financial support from 'Higher Education Commission of Pakistan' through project No. 20-3715/NRPU/R&D/HEC/14/162 and Government College University, Faisalabad, Pakistan. Sadia Sultan would like to acknowledge Universiti Teknologi MARA for the financial support under the reference number UiTM 600- IRMI/FRGS 5/3 (0119/2016) and LESTARI grant 600-RMI/DANA5/3 LESTARI (92/2015). Jamshed Iqbal is thankful to the Organization for the Prohibition of Chemical Weapons (OPCW), The Hague, The Netherlands and Higher Education Commission of Pakistan for the financial support through Project No. 20-3733/NRPU/R&D/14/520.

Conflict of interest

The authors confirm that this article content has no conflict of interest.

References

- [1] R.K.P. Tripathi, V.M. Sasi, S.K. Gupta, S. Krishnamurthy, S.R. Ayyannan, J. Enzyme Inhib. Med. Chem. 33 (2018) 37–57.
- [2] B. Mathew, G.E. Mathew, G. Ucar, M. Joy, E.K. Nafna, J. Suresh, Int. J. Biol. Macromol. 104 (2017) 1321-1329.
- [3] S. Deshwal, M. Di Sante, F. Di Lisa, N. Kaludercic, Curr. Opin. Pharmacol. 33 (2017) 64–69.
- [4] M.C. Costas-Lago, P. Besada, F. Rodríguez-Enríquez, D. Viña, S. Vilar, E. Uriarte, F. Borges, C. Terán, Eur. J. Med. Chem. 139 (2017) 1-11.
- [5] S. Distinto, R. Meleddu, M. Yanez, R. Cirilli, G. Bianco, M.L. Sannaa, A. Arridu, P. Cossu, F. Cottiglia, C. Faggi, F. Ortuso, S. Alcaro, E. Maccioni, Eur. J. Med. Chem. 108 (2016) 542-552.
- [6] Z. Sang, K. Wang, H. Wang, L. Yu, H. Wang, Q. Ma, M. Ye, X. Han, W. Liu, Bioorg. Med. Chem. Lett. 27 (2017) 5053–5059.
- [7] S. Pålhagen, E. Heinonen, J. Häggglund, T. Kaugesaar, O. Mäki-Ikola, R. Palm and the Swedish Parkinson Study Group. Neurology 66 (2006) 1200–1206.
- [8] C. Lu, Y. Guo, J. Yan, Z. Luo, H.-B. Luo, M. Yan, L. Huang, X. Li, J. Med. Chem. 56 (2013) 5843–5859.

- [9] J. Hu, P.A. Ferchmin, A.M. Hemmerle, K.B. Seroogy, V.A. Eterovic, J. Hao, *Front. Neurosci.* 11 (2017) 272-283.
- [10] J. Korábečný, E. Nepovimová, T. Cikánková, K. Špilovská, L. Vašková, E. Mezeiová, K. Kuča, J. Hroudová, *Neuroscience S0306-4522* (2017) 30439-6.
- [11] D. Hea, P. Hua, X. Denga, Z. Song, L. Yuan, X. Yuan, H. Deng, *Neurosci. Lett.* 653 (2017) 351–354.
- [12] J.P.M. Finberg, *Pharmacol. Therapeut.* 143 (2014) 133-152.
- [13] E.D. Deeks, *Drugs* 75 (2015) 705-711.
- [14] S. Carradori, R. Silvestri, *J. Med. Chem.* 58 (2015) 6717-6732.
- [15] S. Distinto, R. Meleddu, M. Yañez, R. Cirilli, G. Bianco, M.L. Sanna, A. Arridu, P. Cossu, F. Cottiglia, C. Faggi, F. Ortuso, S. Alcaro, E. Maccioni, *Eur. J. Med. Chem.* 108 (2016) 542-552.
- [16] Z.V. Chirkova, M.V. Kabanova, S.I. Filimonov, I.G. Abramov, A. Petzer, J.P. Petzer, S.I. Firgang, K.Y. Saponitsky, *Bioorg. Med. Chem. Lett.* 25 (2015) 1206-1211.
- [17] N.T. Tzvetkov, S. Hinz, M. Gastreich, C.E. Müller, *J. Med. Chem.* 57 (2014) 6679-6703.
- [18] M.-H. Nam, M. Park, H. Park, Y. Kim, S. Yoon, V.S. Sawant, J.W. Choi, J.-H. Park, K.D. Park, S.-J. Min, C.J. Lee, H. Choo, *ACS Chem. Neurosci.* 8 (2017) 1519-1529.
- [19] J. Reis, F. Cagide, D. Chavarria, T. Silva, C. Fernandes, A. Gaspar, E. Uriarte, R. Remiao, S. Alcaro, F. Ortuso, F. Borges, *J. Med. Chem.* 59 (2016) 5879-5893.
- [20] M.D. Mertens, S. Hinz, C.E. Müller, M. Gütschow, *Bioorg. Med. Chem.* 22 (2014) 1916-1928.
- [21] J. Joubert, G.B. Foka, B.P. Repsold, D.W. Oliver, E. Kapp, S.F. Malan, *Eur. J. Med. Chem.* 125 (2017) 853-864.
- [22] S. Zaib, S.U.F. Rizvi, S. Aslam, M. Ahmad, M. Al-Rashida, J. Iqbal, *Med. Chem.* 11 (2015) 497-505.
- [23] S. Zaib, S.U.F. Rizvi, S. Aslam, M. Ahmad, S.M.A. Abid, M. Al-Rashida, J. Iqbal, *Med. Chem.* 11 (2015) 580-589.
- [24] S.M.A. Abid, S. Aslam, S. Zaib, S.M. Bakht, M. Ahmad, J.M. Gardiner, J. Iqbal, *Med. Chem. Comm.* 8 (2017) 452-464.
- [25] N. Abbas, S. Zaib, S.M. Bakht, A. Ibrar, I. Khan, S. Batool, A. Saeed, J. Iqbal, *Bioorg. Chem.* 70 (2017) 17-26.
- [26] S.M.A. Abid, H.A. Younus, M. al-Rashida, Z. Arshad, T. Maryum, M.A Gilani, A.I. Alharthi, J. Iqbal, *Bioorg. Chem.* 75 (2017) 291-302.

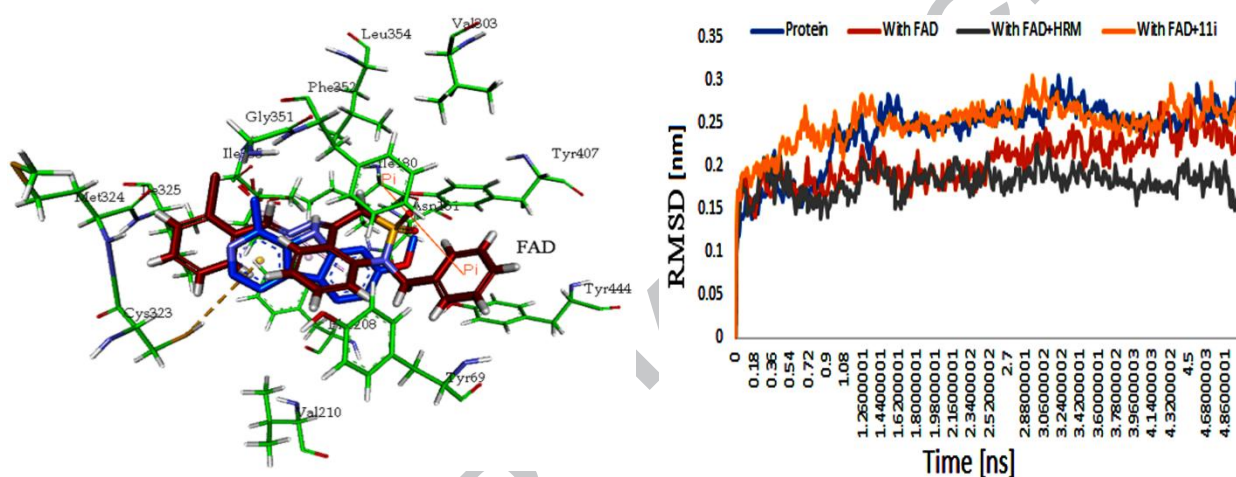
- [27] F.A. Siddique, S. Zaib, S. Jalil, S. Aslam, M. Ahmad, S. Sultan, H. Naz, M. Iqbal, J. Iqbal, *Eur. J. Med. Chem.* 143 (2018) 1373-1386.
- [28] S. Aslam, M. Ahmad, M.M. Athar, U.A. Ashfaq, G.M. Gardiner, C. Montero, M. Detorio, M. Parvez, R.F. Schinazi, *Med. Chem. Res.* 23 (2014) 2930-2946.
- [29] A. Barazarte, G. Lobo, N. Gamboa, J.R. Rodrigues, M.V. Capparelli, A. Alvarez-Larena, S.E. Lopez, J.E. Charris, *Eur. J. Med. Chem.* 44 (2009) 1303-1310.
- [30] M. Pieroni, S. Sabatini, S. Massari, S.W. Kaatz, V. Cecchetti, O. Abarrini, *Med. Chem. Commun.* 3 (2012) 1092-1097.
- [31] M. Shafiq, M. Zia-ur-Rehman, I.U. Khan, M.N. Arshad, S.A. Khan, *J. Chilean Chem. Soc.* 56 (2011) 527-531.
- [32] E.S. Lazer, C.K. Miao, C.L. Cywin, R. Sorcek, H.C. Wong, Z. Meng, I. Potocki, M.A. Hoermann, R.J. Snow, M.A. Tschantz, T.A. Kelly, D.W. McNeil, S.J. Coutts, L. Churchill, A.G. Graham, E. David, P.M. Grob, W. Engel, H. Meier, G. Trummlitz, *J. Med. Chem.* 40 (1997) 980-989.
- [33] I.V. Ukrainets, L.A. Petrushova, S.P. Dzyubenko, G. Sim, *Chem. Heterocycl. Compd.* 50 (2014) 103-110.
- [34] Y. Misu, H. Togo, *Org. Biomol. Chem.* 1 (2003) 1342-1346.
- [35] M. Harmata, N.L. Calkins, R.G. Baughman, C.L. Barnes, *Org. Biomol. Chem.* 71 (2006) 3650-3652.
- [36] P. Yeung, J. Hubbard, E. Korchinski, K. Midha, *Eur. J. Clin. Pharm.* 45 (1993) 563-569.
- [37] K.T. Olkkola, A.V. Brunetto, M. Mattila, *Clin. Pharmacok.* 26 (1994) 107-120.
- [38] S. Grover, L.J. Alderwick, A.K. Mishra, K. Krumbach, J. Marienhagen, L. Eggeling, A. Bhatt, G.S.J. Besra, *J. Bio. Chem.* 289 (2014) 6177-6187.
- [39] A. Rai V. Raj, M.H. Aboumanei, A.K. Singh, A.K. Keshari, S.P. Verma, S. Saha, , *Comb. Chem. High Throughput Screen.* 20 (2017) 658-674.
- [40] Y.P. Gong, R.Z. Wan, Z.P. Liu, *Expert. Opin. Ther. Pat.* 28 (2018) 167-171.
- [41] I.V. Ukrainets, L.A. Petrushova, L.V. Sidorenko, A.A. Davidenko, M.A. Duchenko, *Sci. Pharm.* 84 (2016) 497-506.
- [42] A. Mancini, A. Chelini, A. Di Capua, L. Castelli, S. Brogi, M. Paolino, G. Giuliani, A. Cappelli, M. Frosini, L. Ricci, E. Leonelli, G. Giorgi, A. Giordani, J. Magistretti, M. Anzini, *Eur. J. Med. Chem.* 126 (2017) 614-630.
- [43] A. Shabbir, M. Shahzad, A. Ali, M. Zia-Ur-Rehman, *Inflammation.* 39 (2016) 1918-1929.

- [44] W.Z. Jia, F. Cheng, Y.J. Zhang, J.Y. Ge, S.Q. Yao, Q. Zhu, *Chem. Biol. Drug Des.* 89 (2016) 141-151.
- [45] S.Y. Son, J. Ma, Y. Kondou, M. Yoshimura, E. Yamashita, T. Tsukihara, *Proc. Nat. Acad. Sci.* 105 (2008) 5739-5744.
- [46] C. Binda, J. Wang, L. Pisani, C. Caccia, A. Carotti, P. Salvati, D.E. Edmondson, A. Mattevi, *J. Med. Chem.* 50 (2007) 5848-5852.
- [47] C. Binda, M. Li, F. Hubàlek, N. Restelli, D.E. Edmondson, A. Mattevi, *Proc. Nat. Acad. Sci.* 100 (2003) 9750-9755.
- [48] <http://www.simulations-plus.com>
- [49] P. Stenberg, U. Norinder, K. Luthman, P. Artursson, *J. Med. Chem.* 44 (2001) 1927-1937.
- [50] H. Van de Waterbeemd, E. Gifford, *Nat. Rev. Drug Discov.* 2 (2003) 192-204.
- [51] P. Zakeri-Milani, H. Tajerzadeh, Z. Islambolchilar, S. Barzegar, H. Valizadeh, *DARU* 14 (2006) 164-171.
- [52] K. Asokkumar, L.T. Prathyusha, M. Umamaheshwari, T. Sivashanmugam, V. Subhandradevi, P. Jagannath, A. Madeswaran, F. Salesheir, *J. Chil. Chem. Soc.* 57 (2012) 1442-1446.
- [53] D.E. Clark, S.D. Pickett, *Drug Discov. Today.* 5 (2000) 49-58.
- [54] M. Shafiq, I.U. Khan, M.N. Arshad, W.A. Siddiqui, *Asian. J. Chem.* 23 (2011) 2101.

Graphical Abstract

Synthesis, characterization, monoamine oxidase inhibition, molecular docking and dynamic simulations of novel 2,1-benzothiazine-2,2-dioxide derivatives

Shakeel Ahmad, Sumera Zaib, Saquib Jalil, Muhammad Shafiq, Matloob Ahmad, Sadia Sultan, Mazhar Iqbal, Sana Aslam, Jamshed Iqbal*



Molecular docking and dynamic simulations of novel 2,1-benzothiazine-2,2-dioxide derivative as potent and selective monoamine oxidase A inhibitor

Research Highlights

- Three series of novel 2,1-benzothiazine-2,2-dioxide were synthesized.
- Potent and selective inhibitors of monoamine oxidases were revealed.
- Molecular docking studies further supported the in vitro results.
- Dynamic simulations and HYDE assessment were explored for potent inhibitors of MAO-A & MAO-B.
- Compounds exhibited favorable ADME profile with good oral bioavailability.